# Two-dimensional model of phase segregation in liquid binary mixtures

Natalia Vladimirova,[1] Andrea Malagoli,[2] and Roberto Mauri[1]
[1]*Department of Chemical Engineering, The City College of CUNY, New York, New York 10031*
[2]*Department of Astronomy and Astrophysics, University of Chicago, Chicago, Illinois 60637*
(Received 6 August 1998; revised manuscript received 26 July 1999)

The hydrodynamic effects on the late stage kinetics of phase separation in liquid mixtures is studied using the model *H*. Mass and momentum transport are coupled via a nonequilibrium body force, which is proportional to the Peclet number $\alpha$, i.e., the ratio between convective and diffusive molar fluxes. Numerical simulations based on this theoretical model show that phase separation in low viscosity, liquid binary mixtures is mostly driven by convection, thereby explaining the experimental findings that the process is fast, with the typical size of single-phase domains increasing linearly with time. However, as soon as sharp interfaces form, the linear growth regime reaches an end, and the process appears to be driven by diffusion, although the condition of local equilibrium is not reached. During this stage, the typical size of the nucleating drops increases like $t^n$, where $\frac{1}{3}<n<\frac{1}{2}$, depending on the value of the Peclet number. As the Peclet number increases, the transition between convection- and diffusion-driven regimes occurs at larger times, and therefore for larger sizes of the nucleating drops. [S1063-651X(99)10611-1]

PACS number(s): 64.70.Ja, 64.60.Cn, 64.60.Ht, 64.75.+g

## I. INTRODUCTION

The main objective of this work is to determine whether the linear growth regime of phase separating liquid mixtures can continue indefinitely with time or if it reaches an end, finding the connection between the morphology of the system and its growth rate. When a binary mixture is quenched from its single-phase region to a temperature below the composition-dependent spinodal curve, it phase separates [1]. This process, called spinodal decomposition, is characterized by the spontaneous formation of single-phase domains which then proceed to grow and coalesce. Unlike nucleation, where an activation energy is required to initiate the separation, spinodal decomposition involves the growth of any fluctuations whose wavelength exceeds a critical value. Experimentally, the typical domain size is described by a power-law time dependence $t^n$, where $n\approx 1/3$ when diffusion is the dominant mechanism of material transport, while $n\approx 1$ when hydrodynamic, long-range interactions become important [2–4].

Dimensionally, all possible scaling of the process were summarized by Furukawa [5], showing in particular that when hydrodynamic forces are taken into account, the growth laws $R(t)\sim(\sigma/\eta)t$ and $R(t)\sim(\sigma/\rho)^{1/3}t^{2/3}$ can be obtained, depending on whether the surface tension $\sigma$ is balanced by viscous or inertial forces, with $\eta$ and $\rho$ denoting the typical viscosity and density of the mixture, respectively. A growth exponent $n\sim 5/3$ is also associated with inertia, but it seems less relevant, as it has never been observed in experiments or in numerical simulations.

In previous large scale molecular dynamics simulations [6,5], it was shown that the late time dynamics of spinodal decomposition reaches a viscous scaling regime with a growth exponent $n=1$, while $n=2/3$ is obtained in the inertial regime [7,8]. Similar results were obtained using lattice-Boltzmann simulations [9]. Molecular dynamics and lattice-Boltzmann simulations, however, can only model systems of very small sizes and/or for very short times, while in this work, we intend to study the behavior of phase separating systems at later times, that is when the typical size of the single-phase domains is of $O(1\ \mu\mathrm{m})$. Therefore, we must use the third numerical approach that is generally applied to study the phase separation of liquid mixtures, namely, numerical integration of the coarse-grained conservation equation, generally referred to as model *H*, in the taxonomy of Halperin and Hohenberg [10].

Model *H* is based on the Ginzburg-Landau theory of phase transition [11], which was applied to model the phase separation of mixtures by Cahn and Hilliard [12] and later generalized to include hydrodynamics by Kawasaki [13]. In this model, the equations of conservation of mass and momentum are coupled via the convective term of the convection-diffusion equation, which is driven by a composition-dependent body force. As noted by Jasnow and Viñals [14], when the system is composed of single-phase domains separated by sharp interfaces, this force incorporates capillary effects, and plays the role of a Marangoni force. Model *H* shows that during the early stages of the phase separation process (i.e., spinodal decomposition), initial instabilities grow exponentially, forming, at the end, single-phase microdomains whose size corresponds to the fastest-growing mode $\lambda_0$ of the linear regime [15]. During the late stages of the process, i.e., for times $t>\tau_0=\lambda_0^2/D$, where $D$ is the molecular diffusivity, the system consists of well-defined patches in which the average concentration is not too far from (albeit not equal to) its equilibrium value [16]. At this point, material transport can occur either by diffusion or by convection. In cases where diffusion is the only transport mechanism, both analytical calculations [17] and dimensional analysis [18] predict a growth law $R(t)\sim t^{1/3}$, due to the Brownian coagulation of droplets. On the other hand, when hydrodynamic interactions among droplets become important, the effect of convective mass flow resulting from surface tension effects can no longer be neglected. In this case, both dimensional analysis [18,19] and numerical simulation [19–22] indicate that viscous forces determine a

 

growth law $R(t)\sim t$. On the other hand, when inertia is dominant, the growth rate is described in terms of an exponent $n\approx 2/3$ [23–25]. Recently, Tanaka and Araki [26] showed that the scaling exponent for the domain growth is not universal, and depends on the relative importance of hydrodynamic flow and diffusion.

In this work we continue to explore the influence of convection upon phase segregation in fluid mixtures, applying an extension of model *H* which leads to an easily integrable set of equations. Adopting a larger system than that of previous investigators' [19–22], we showed that the linear growth regime does not continue *ad infinitum* in time: as soon as sharp interfaces form, the system reaches a metastable state, where diffusion is the driving force, characterized by a much slower growth rate. In addition, the morphology of the system appears to change drastically when the Peclet number increases from $10^2$ to $10^4$.

## II. GOVERNING EQUATIONS

### A. Binary mixture at equilibrium

Consider a homogeneous mixture of two species *A* and *B* with molar fractions $x_A=\phi$ and $x_B=1-\phi$, respectively, kept at temperature *T* and pressure *P*. For the sake of simplicity, in our model we assume that the molecular weights, specific volumes, and viscosities of *A* are equal to those of *B*, namely, $M_A=M_B=M_W$, $\overline{V}_A=\overline{V}_B=\overline{V}$, and $\eta_A=\eta_B=\eta$, respectively, so that molar, volumetric, and mass fractions are all equal to each other, and the mixture viscosity is composition independent. The equilibrium state of this system is described by the ''coarse-grained'' free energy functional, that is the molar Gibbs energy of mixing, $\Delta g_{\rm eq}$,

$$\Delta g_{\rm eq}=g_{\rm eq}-(g_A x_A+g_B x_B), \tag{1}$$

where $g_{\rm eq}$ is the energy of the mixture at equilibrium, while $g_A$ and $g_B$ are the molar free energy of pure species *A* and *B*, respectively, at temperature *T* and pressure *P*. The free energy $\Delta g_{\rm eq}$ is the sum of an ideal, entropic part and an enthalpic part,

$$\Delta g_{\rm eq}=RT[\phi\ln\phi+(1-\phi)\ln(1-\phi)]+RT\Psi\phi(1-\phi), \tag{2}$$

where *R* is the gas constant, while $\Psi$ is a function of *T* and *P*. This expression, which is generally referred to as either the Flory-Huggins free-energy density [27] or the one-parameter Margules correlation [28], is generally derived by considering the molecular interactions between nearest neighbors [29], or summing all pairwise interactions throughout the whole system [30]. Equation (2) can also be derived from first principles, assuming that the *A*-*A* and *B*-*B* intermolecular forces are equal to each other and larger than the *A*-*B* intermolecular forces, i.e., $F_{AA}=F_{BB}>F_{AB}$, obtaining an expression for $\Psi$ which depends on $(F_{AA}$-$F_{AB})$ [15]. In the following, we shall assume that *P* is fixed, so that the physical state of the mixture at equilibrium depends only on *T* and $\phi$.

In order to take into account the effects of spatial inhomogeneities, Cahn and Hilliard [12] introduced the generalized specific free energy *g*, which is given by the expression

$$g=g_{\rm eq}+\tfrac{1}{2}RTa^2(\nabla\phi)^2, \tag{3}$$

where *a* represents the typical length of spatial inhomogeneities in the composition. As shown by van der Waals [31], since the surface tension $\sigma$ is the energy stored in the unit area of the interface separating two phases at local equilibrium, we obtain

$$\sigma=\frac{1}{2}\frac{\rho RT}{M_W}a^2\int(\nabla\phi)^2dl\sim\frac{\rho RTa}{M_W}(\Delta\phi)_{\rm eq}^2\sqrt{\Psi-2}, \tag{4}$$

where $(\Delta\phi)_{\rm eq}=(\phi_1-\phi_2)_{\rm eq}$ is the concentration drop across the interface, while we have considered that the width of the interface *l* equals the wavelength corresponding to the fastest growing mode of the linear regime [15], $l\sim a/\sqrt{\Psi-2}$. For a typical liquid mixture near its miscibility curve we obtain $a\sim 0.1\ \mu$m.

Below a certain critical temperature $T_c$, corresponding to values $\Psi\geqslant 2$, the molar free energy given by Eq. (2) is a double-well potential, and therefore a first-order phase transition will take place. Now it is well known that the molar free energy can be written as [28]

$$g_{\rm eq}/RT=\mu\phi, \tag{5}$$

where $\mu=(\mu_A-\mu_B)$ denotes the difference between the chemical potential of species *A* and *B* in solution, respectively. This result can be extended [12] defining the generalized chemical potential $\tilde{\mu}$,

$$\tilde{\mu}=\frac{\delta(g/RT)}{\delta\phi}=\frac{\partial(g/RT)}{\partial\phi}-\boldsymbol{\nabla}\cdot\frac{\partial(g/RT)}{\partial(\boldsymbol{\nabla}\phi)}, \tag{6}$$

and substituting Eqs. (1)–(3) into Eq. (6), we obtain

$$\tilde{\mu}=\mu_o+\ln\frac{\phi}{1-\phi}+\Psi(1-2\phi)-a^2\nabla^2\phi, \tag{7}$$

where $\mu_o=(g_B-g_A)/RT$.

### B. Equations of motion

Imposing that the number of particles of each species is conserved, we obtain the continuity equations [32]

$$\frac{\partial c_A}{\partial t}+\boldsymbol{\nabla}\cdot(c_A\mathbf{v}_A)=0, \tag{8}$$

$$\frac{\partial c_B}{\partial t}+\boldsymbol{\nabla}\cdot(c_B\mathbf{v}_B)=0, \tag{9}$$

where $c_A$ and $c_B$ are the concentrations, while $\mathbf{v}_A$ and $\mathbf{v}_B$ are the mean velocities of species *A* and *B*, respectively. For an incompressible mixture composed of species with equal physical properties, Eqs. (8) and (9) lead to the following continuity equations in terms of the mass fraction $\phi$ of the *A* species (which is equal to its mole fraction):

$$\frac{\partial\phi}{\partial t}+\mathbf{v}\cdot\boldsymbol{\nabla}\phi=-\frac{1}{\rho}\boldsymbol{\nabla}\cdot\mathbf{j}, \tag{10}$$

$$\boldsymbol{\nabla}\cdot\mathbf{v}=0, \tag{11}$$

where $\rho$ is the mixture mass density, $\mathbf{j}=\rho\phi(1-\phi)(\mathbf{v}_A-\mathbf{v}_B)$ is the diffusive mass flux, and $\mathbf{v}$ is the average velocity of the mixture, $\mathbf{v}=x_A\mathbf{v}_A+x_B\mathbf{v}_B$. The velocities $\mathbf{v}_A$ and $\mathbf{v}_B$ are the sums of a convective part $\mathbf{v}$ and a diffusive part,

$$\mathbf{v}_A=\mathbf{v}-D\nabla\mu_A, \quad \mathbf{v}_B=\mathbf{v}-D\nabla\mu_B, \tag{12}$$

where $D$ is a composition-independent diffusion coefficient, and we have assumed that the diffusive parts of $\mathbf{v}_A$ and $\mathbf{v}_B$ are proportional to the gradients of the chemical potentials (see Refs. [33,34] for a justification of this assumption). Consequently, the diffusive flux becomes

$$\mathbf{j}=-\rho\phi(1-\phi)D\nabla\tilde{\mu}. \tag{13}$$

Finally, substituting (7) into (13), we obtain

$$\frac{\mathbf{j}}{\rho}=-D\nabla\phi+D\phi(1-\phi)[a^2\nabla\nabla^2\phi+2\Psi\nabla\phi+(2\phi-1)\nabla\Psi]. \tag{14}$$

This expression for $\mathbf{j}$ coincides with that used in Ref. [15]. The term $D\nabla\phi$ in Eq. (14) represents the regular diffusion flux, while the last term vanishes for small concentrations of either solvents ($\phi\to0$ or $\phi\to1$) and for ideal mixtures ($a=\Psi=0$). Note that the $a^2$ term is always stabilizing, and is relevant only at small length scales, while $\Psi$ is a known function of the temperature, and near the critical temperature $T_c$ it is proportional to $T_c-T$.

If the flow is slow enough that the dynamic terms in the Navier-Stokes equation can be neglected, conservation of momentum leads to the Stokes equation

$$\eta\nabla^2\mathbf{v}-\nabla p=-\mathbf{F}_\phi, \tag{15}$$

where $\eta$ is the mixture viscosity, which, we assume, is composition independent, while $\mathbf{F}_\phi$ is a body force, which equals the gradient of the free energy [10], and therefore is driven by the concentration gradients within the mixture [25,14,5]

$$\mathbf{F}_\phi=\frac{\rho}{M_W}\nabla g=\left(\frac{\rho RT}{M_W}\right)\tilde{\mu}\nabla\phi. \tag{16}$$

The assumption of small Reynolds number is supported by the experimental observation [35] that during phase separation of liquid mixtures with waterlike viscosity 10 $\mu$m drops move at speeds exceeding 200 $\mu$m/s. At equilibrium, where the free energy is uniform, the body force $\mathbf{F}_\phi$ is zero, and therefore there cannot be any convection. In addition, when the mixture is composed of well-defined single-phase domains separated by a thin interface located at $\mathbf{r}=\mathbf{r}_s$, the body force $\mathbf{F}_\phi$ can be interpreted as a capillary force at $\mathbf{r}_s$, i.e. [14],

$$\mathbf{F}_\phi(\mathbf{r})=[\hat{\mathbf{n}}\sigma\kappa+(\mathbf{I}-\hat{\mathbf{n}}\hat{\mathbf{n}})\cdot\nabla\sigma]\delta(\hat{\mathbf{n}}\cdot(\mathbf{r}-\mathbf{r}_s)), \tag{17}$$

where $\sigma$ is the surface tension, while $\hat{\mathbf{n}}$ and $\kappa$ are the unit vector perpendicular to the interface and the curvature at $\mathbf{r}_s$, respectively. Physically, $\mathbf{F}_\phi$ tends to minimize the energy stored at the interface, and therefore it drives, say, $A$-rich drops toward $A$-rich regions, enhancing coalescence. Note that Eq. (15) can also be written as

$$\eta\nabla^2\mathbf{v}-\nabla p'=\left(\frac{\rho RT}{M_W}\right)\phi\nabla\tilde{\mu}, \tag{18}$$

with $p'=p-(\rho RT/M_W)\tilde{\mu}\phi$. Equations (10), (11), and (18) constitute the so-called model $H$ [10].

Now we restrict our analysis to two-dimensional systems, so that the velocity $\mathbf{v}$ can be expressed in terms of a stream function $\psi$, i.e., $v_1=\partial\psi/\partial r_2$ and $v_2=-\partial\psi/\partial r_1$. Consequently, substituting Eq. (16) into Eq. (15), we obtain

$$\frac{\partial\phi}{\partial t}=\nabla\psi\times\nabla\phi+\frac{1}{\rho}\nabla\cdot\mathbf{j}, \tag{19}$$

$$\eta\nabla^4\psi=\nabla\mu\times\nabla\phi, \tag{20}$$

where

$$\mathbf{A}\times\mathbf{B}=A_1B_2-A_2B_1.$$

Since the main mechanism of mass transport at the beginning of phase segregation is diffusion, the length scale of the process is the microscopic length $a$. Therefore, using the scaling

$$\tilde{r}=\frac{1}{a}r, \quad \tilde{t}=\frac{D}{a^2}t, \quad \tilde{\psi}=\frac{1}{\alpha D}\psi, \tag{21}$$

and substituting Eq. (14) into Eq. (19), we obtain

$$\frac{\partial\phi}{\partial\tilde{t}}=\alpha\tilde{\nabla}\tilde{\psi}\times\tilde{\nabla}\phi+\tilde{\nabla}\cdot(\tilde{\nabla}\phi-\phi(1-\phi)[2\Psi+\tilde{\nabla}^2]\tilde{\nabla}\phi), \tag{22}$$

$$\tilde{\nabla}^4\tilde{\psi}=-\tilde{\nabla}(\tilde{\nabla}^2\phi)\times\tilde{\nabla}\phi, \tag{23}$$

where

$$\alpha=\frac{a^2}{D}\frac{\rho}{\eta}\frac{RT}{M_W}. \tag{24}$$

The nondimensional number $\alpha$ is the ratio between thermal and viscous forces, and can be interpreted as the Peclet number, that is the ratio between convective and diffusive mass fluxes in the convection-diffusion equation (22), i.e., $\alpha=Va/D$. Here $V$ is a characteristic velocity, which can be estimated through Eqs. (15) and (16) as $V\sim F_\phi a^2/\eta=\alpha D/a$, where $F_\phi\sim\rho RT/(aM_W)$. A similar, so called ''fluidity'' parameter was also defined by Tanaka and Araki [26]. For systems with very large viscosity, $\alpha$ is small, so that the model describes the diffusion-driven separation process of polymer melts and alloys [15]. For most liquids, however, $\alpha$ is very large, with typical values ranging from $10^3$ to $10^5$. Therefore, it appears that diffusion is important only at the very beginning of the separation process, in that it creates a nonuniform concentration field. Then the concentration-gradient-dependent capillary force induces the convective material flux which is the dominant mechanism for mass transport. At no time, however, can the diffusive term in Eq. (15) be neglected, as it stabilizes the interface and saturates the initial exponential growth. In addition, it should be stressed that the stream function $\psi$ depends on

high order derivatives of the concentration and therefore it is very sensitive to the concentration profile within the interface.

### III. NUMERICAL RESULTS

The governing equations (22) and (23) were solved on a uniform two-dimensional square grid with constant width $[(x_i,y_j)=(i\Delta x,j\Delta y),i=1,N,j=1,N]$, where $N=500$, and time discretization $[t=n\Delta t,n=0,1,2,\ldots]$. The physical dimensions of the grid were chosen such that $\Delta x/a,\Delta y/a=2$, while the time step $\Delta t$ satisfies $\Delta t/(a^2/D)\approx 0.1$–$0.001$. The choice of the time step $\Delta t$ was determined semiempirically in order to maintain the stability of the numerical scheme. Note that the nonlinearity of the equations prevents a rigorous derivation of the stability constraints on $\Delta t$, but one can roughly estimate that the size of $\Delta t$ will scale as $O(\Delta x^4,\Delta y^4)$, which is the order of the highest operator in the discretized system. The space discretization was based on a cell-centered approximation of both the concentration variable $\phi_{ij}^n(t)$ and of the stream function $\psi$. The spatial derivatives in the right-hand side of Eqs. (22) and (23) were discretized using a straightforward second-order accurate approximation. The time integration from $t^n=n\Delta t$ to $t^{n+1}=(n+1)\Delta t$ was achieved in two steps. First, we computed the stream function $\psi$ by solving the biharmonic equation (23) with the source term evaluated at time $t^n=n\Delta t$. The biharmonic equations was solved using the DBIHAR routine from netlib [36]. Second, Eq. (22) was advanced in time, using the velocity field computed from the updated stream function and a straightforward explicit Eulerian step. This makes the entire scheme $O(\Delta t)$ accurate in time, which is acceptable for our problem, since the size of the time step is kept very small anyway by the stability constraints. The boundary conditions were no flux for the concentration field and no slip for the velocity field. The discretization of the derivatives near the boundaries was modified to use only interior points. In general, our results are not very sensitive to the precise treatment of boundary conditions, since the gradients remain close to zero near the boundaries.

Since we did not incorporate thermal noise into our simulation, we introduced some amount of randomness into the system through a background noise in the concentration field, $\delta\phi$, with $\langle\delta\phi\rangle=0$ and $\langle(\delta\phi)^2\rangle^{1/2}=0.01$, which was uncorrelated both in space and in time. That means that at each time step a spatially uncorrelated noise was added to the concentration field, and was then subtracted at the next time step, only to be replaced with another spatially uncorrelated background noise of the same amplitude [16]. This procedure which is equivalent to adding noise to the flux $\mathbf{j}$ on the right hand side of Eq. (10), is fully conservative in the sense that the volume integral of the composition $\phi$ is not altered by addition of the *ad hoc* noise (numerically we have verified that the composition is indeed conserved to machine accuracy). In a separate set of numerical simulations, thermal fluctuations were included in the initial conditions only, as in Furukawa [5], obtaining identical results. In other simulations, the physical thermal noise was used, satisfying the fluctuation-dissipation theorem [25], again obtaining identical results. In fact, since for deep quenches the Ginzburg inequality is satisfied [11], the background noise does not affect the behavior of the system, and only determines the instant of time when the system departs from its initial uniform state (see Fig. 7 in Vladimirova *et al.* [16]): once the linear regime is reached, the presence of the noise becomes irrelevant.

Both critical and off-critical quenches were considered, with uniform initial concentration fields $\phi_0=0.5$ and 0.45, respectively. The boundary conditions were no flux for the concentration field and no slip for the velocity field. In most of our simulations we used $\Psi=2.1$, because this is the Margules parameter of the water-acetonitrile-toluene mixture with 20 °C temperature quench that we used in our experimental study [35]. However, simulations with different values of $\Psi$ were also performed, obtaining very similar results. Note that, for $\Psi=2.1$, at equilibrium the two phases have compositions $\phi_{\rm eq}^A=0.685$ and $\phi_{\rm eq}^B=0.315$. Time was measured as $t=(10^5a^2/D)\tau$, where $\tau$ is a nondimensional time. Since typical values of $D$ and $a$ are $10^{-5}$ cm$^2$/s and $10^{-5}$ cm, respectively, then $\tau\sim t/(1s)$.

First, we solved Eqs. (22) and (23) for a system with critical uniform initial mole fraction $\phi_0=0.5$ and for different values of the Peclet number $\alpha$. The first row of images in Fig. 1 represents the results for $\alpha=0$, e.g., for the case when diffusion is the only mechanism of mass transfer, showing that, soon after the first drops appear, they coalesce into dendroidlike structures. The mean composition within (and without) these structures changes rapidly, as at time $\tau=0.05$ we already see two clearly distinguishable phases with almost uniform concentrations equal to 0.59 and 0.41. After this early stage, the structures start to grow, increasing their thickness and reducing the total interface area, while at the same time the composition within the domains approaches its equilibrium value. This, however, is a slow process, driven only by diffusion, and at time $\tau=0.1$ the phase domains still have a dendroidlike geometry with a characteristic width which is just twice as large as its initial value. In the following, we will denote these slow-changing configurations as metastable states, referring to Refs. [16,37] for further informations on their evolution.

For nonzero convection, i.e., for $\alpha\neq 0$, dendritic structures thicken faster, but up to $\alpha\approx 10^2$ domain growth still follows the same pattern as for $\alpha=0$: first, single-phase domains start to appear, separated from each other by sharp interfaces, and only later these structures start to grow, with increasing growth rate for larger $\alpha$. When $\alpha>10^2$, however, phase separation occurs simultaneously with the growth process. For example, when $\alpha=10^4$, we see the formation of isolated drops of both phases, surrounded by the bulk of the fluid mixture, which is still not separated. In addition, drops appear to move fast and randomly while they grow, absorbing material from the bulk, colliding with each other and coalescing, so that single-phase domains grow much faster than when molecular diffusion is the only transport mechanism. Consider, for example, the morphology of the system at time $\tau=0.1$ for $\alpha=10^4$ and 0: in the first case, single-phase domains have already reached a size comparable to that of the container's, while, in the absence of convection, the dendroid domains have an approximate width of $20a$. Clearly, since the motion of the interface is too quick for the concentration diffusion to establish a metastable state within

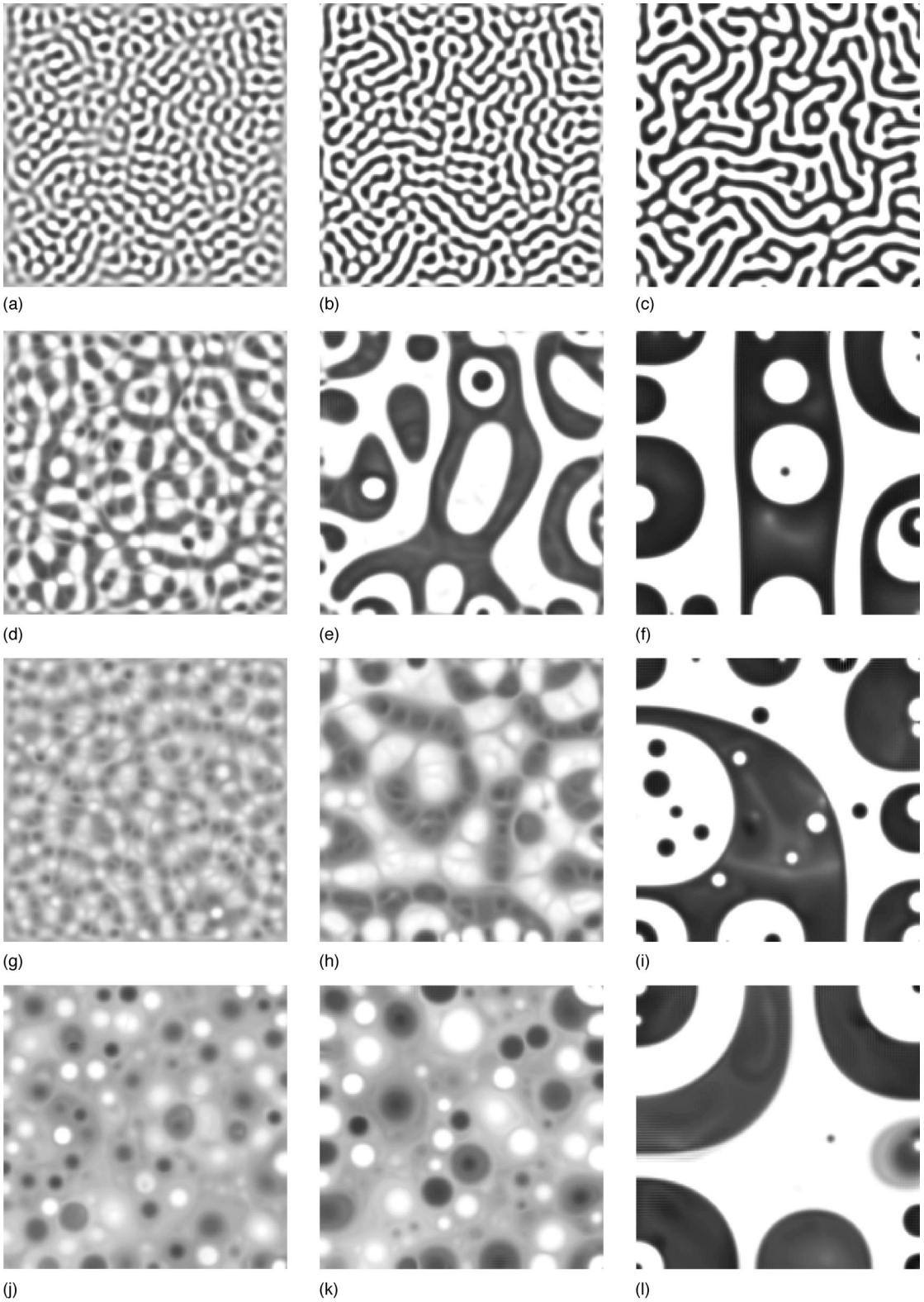


FIG. 1. Composition of a binary mixture at different times $\tau$ after an instantaneous quenching with $\Psi=2.1$ and $\phi_0=0.5$, when the Peclet number $\alpha$ is 0, $10^2$, $10^3$, and $10^4$. The size of the system is $400a\times400a$, with no flux boundary conditions. The snapshots correspond to $\tau=0.04$, 0.05, and 0.10, expressed in $10^5a^2/D$ units. The gray level varies linearly between black and white, corresponding to concentrations $\phi=\phi_{\mathrm{eq}}^A$ and $\phi=\phi_{\mathrm{eq}}^B$, respectively.

the microdomains, double, or multiple, phase separation is observed, in agreement with previous numerical [26,14] and experimental [35,38] results.

Although the dynamics of phase separation in fluids is mostly driven by convection, for very short times the convective driving force $\mathbf{F}_\phi$ is negligible, as composition gradients did not develop yet, and therefore diffusion is the only mechanism of mass transport. In fact, the two pictures in Fig.

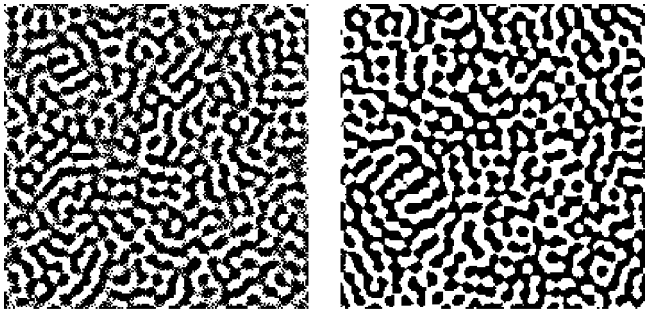


FIG. 2. Concentration field after an instantaneous quenching with $\Psi=2.1$ and $\phi_0=0.5$ at time $t=0.02\times10^5a^2/D$, when the Peclet number $\alpha$ is 0 and $10^4$. The size of the system is $400a\times400a$, with no flux boundary conditions. Black pixels correspond to concentrations $\phi<\phi_0$, and white ones to $\phi>\phi_0$.

2 show that at time $\tau=0.02$ the concentration fields for $\alpha=0$ and $10^4$ are almost indistinguishable from each other, with patterns having a characteristic period $\lambda$ equal to the fastest growing mode in the linear regime for a diffusion-driven process [15], i.e.,

$$\lambda=\frac{2\pi a}{\sqrt{\Psi-2}}. \tag{25}$$

A similar behavior was observed for an off-critical phase separating mixture with $\phi_0=0.45$ (see Fig. 3). As in the critical case, the system tends to form larger single-phase domains as the convection coefficients $\alpha$ increases. Again, while for smaller $\alpha$ the processes of separation and growth occur successively in time, for larger $\alpha$ they occur simultaneously. However, while for critical mixtures the separating phases tend to form interconnected domains, for off-critical mixtures we observe the formation of isolated, mostly circular drops, with no detectable double phase separation. The larger $\alpha$ is, the shorter the relaxation time of a drop after a collision, so that for $\alpha>10^2$ we practically do not observe any noncircular drops.

As a quantitative characterization of the influence of the convection parameter $\alpha$ on the average phase composition within the phase domains, we define the separation depth $s$, measuring the ''distance'' of the single-phase domains from their equilibrium state, i.e.,

$$s=\left\langle\frac{\phi(\mathbf{r})-\phi_0}{\phi_{\rm eq}(\mathbf{r})-\phi_0}\right\rangle,\quad \text{with}\ \ 0\leqslant s\leqslant1, \tag{26}$$

where $\phi_0$ is the initial composition, and the bracket indicates volume and ensemble average. Here $\phi_{\rm eq}$ is the steady state composition of the $A$-rich phase, $\phi_{\rm eq}^A$, or the $B$-rich phase, $\phi_{\rm eq}^B$, depending on the local composition $\phi(\mathbf{r})$,

$$\phi_{\rm eq}(\mathbf{r})=\phi_{\rm eq}^A,\quad \phi(\mathbf{r})>\phi_0, \tag{27}$$

$$\phi_{\rm eq}(\mathbf{r})=\phi_{\rm eq}^B,\quad \phi(\mathbf{r})<\phi_0, \tag{28}$$

so that $s=1$ indicates that the system is a condition of local equilibrium. In Figs. 4 and 5 the separation depth $s$ is plotted as a function of time for both critical and off-critical mixtures. The data points represented in these figures were obtained using a domain size $L=1000a$; however, identical results were obtained with $L=400a$, indicating that they do not depend on the size of the domain nor on the averaging procedure.

As we see in Fig. 4, after a critical quench no detectable phase separation takes place until $\tau\sim0.02$, when the first spinodal decomposition pattern is formed. Then phase separation can take place in two different ways, depending on whether $\alpha<10^2$ or $\alpha>10^3$. For smaller $\alpha$'s, single-phase domains develop very rapidly, until, at $\tau\sim0.06$, they appear to be separated by sharp interfaces. From that point on, separation proceeds much more slowly, as the concentration gradients within the single-phase domains are very small, while the concentrations of the two phases across any interface change only slowly in time (see the discussion in Ref. [16]). Although Tanaka [38] denoted these states as ones of local equilibrium, here we prefer to use the term ''metastable states,'' considering that at stable equilibrium we should have $s=1$, while here we have $s\leqslant0.8$. In the case of larger $\alpha$, with $\alpha>10^3$, the growth of the separation depth is more gradual, revealing that separation and growth occur simultaneously and with no detectable metastable states, although obviously, at some later stage, sharp interfaces will eventually appear even in this case. Therefore, we may conclude that (a) the larger $\alpha$ is, the longer it takes for sharp interfaces to form, and (b) local equilibrium (with $s=1$) is probably never achieved for low-viscosity liquid mixtures. In this case, in fact, $a\sim10^{-5}$ cm, and consequently our domain size corresponds to 100 $\mu$m, while drops start sedimenting when they reach 1-mm sizes, so that the system will become gravity driven and rapidly separate before reaching the scaling regime, with $s=1$.

For off-critical mixtures, as shown in Fig. 5, the onset of phase separation occurs at later times than in the critical case. In particular, the closer $\phi_0$ is to the spinodal concentration $\phi_s$ (in our case, with $\Psi=2.1$, $\phi_s=0.388$), the longer it takes for the onset of phase separation. In addition, for off-critical mixtures the processes of separation and growth tend to occur successively in time, even at high values of the Peclet number. For example, comparing Figs. 4 and 5, we see that, for $\alpha=10^3$, the two processes occur simultaneously in the critical case, and sequentially in the off-critical one. That means that off-critical mixtures are more likely to reach a metastable state, after which single-phase domains grow much more slowly.

The behavior of a phase-separating system depends as much on the driving force $\mathbf{F}_\phi$ as on the Peclet number $\alpha$. Consider, for example, the behavior of two systems with Peclet numbers $\alpha=0$ and $10^3$. In Fig. 4 we see that, at time $\tau=0.08$ and with the same $s=0.6$, the system with $\alpha=0$ is in a metastable state, while that with $\alpha=10^3$ is still in the domain forming, separating stage. In fact, although the capillary driving force $\mathbf{F}_\phi$ is the same in the two cases (as it is a function of the separation depth $s$), it can induce a strong convection only for systems with small viscosities (i.e., large $\alpha$'s), while for very viscous systems it has hardly any effect.

Finally, the equivalent average radius of the drops, $R$, is plotted in Fig. 6 as a function of time, with

$$R=\sqrt{\langle A\rangle/\pi}, \tag{29}$$

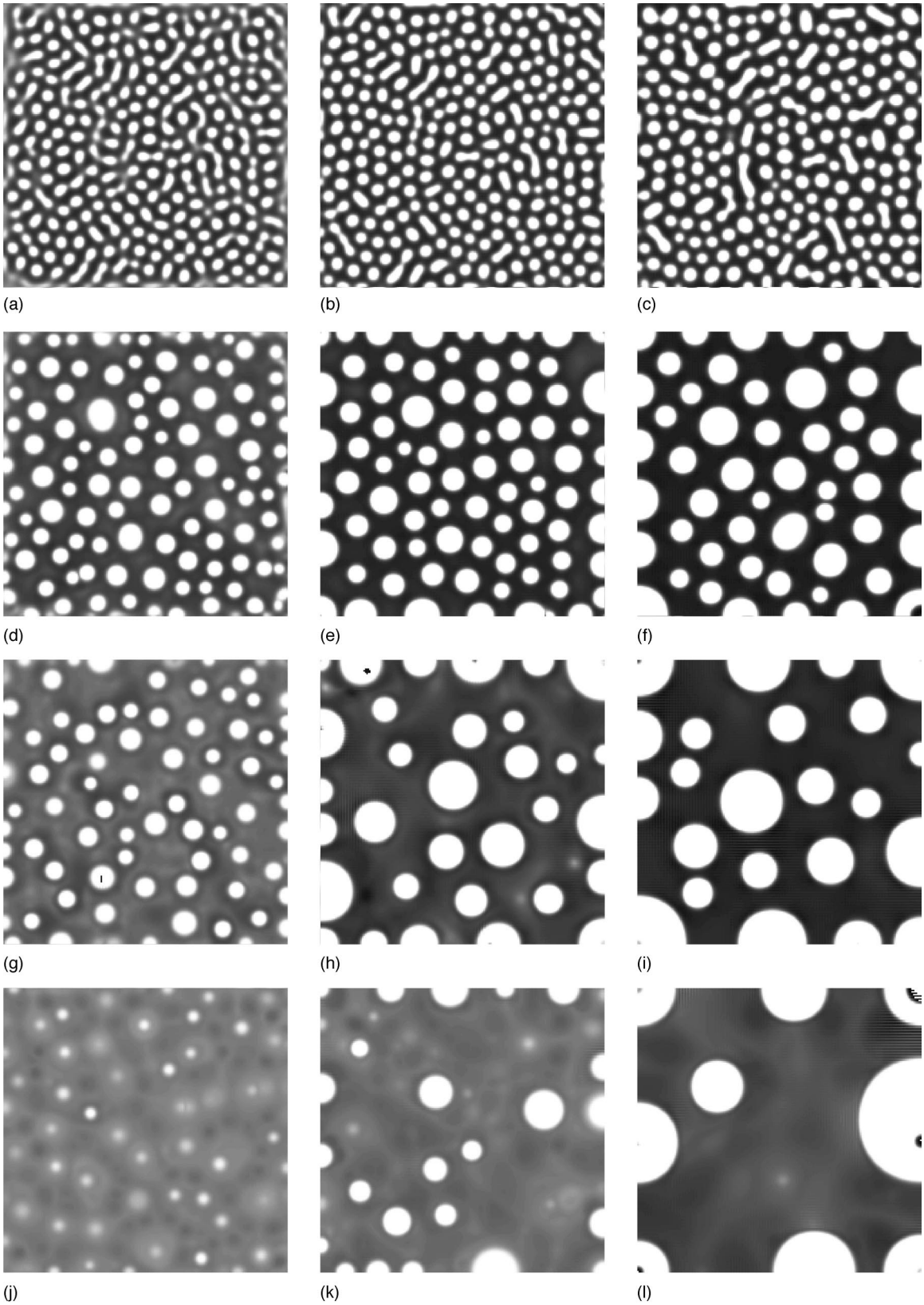


FIG. 3. Composition of a binary mixture at different times $\tau$ after an instantaneous quenching with $\Psi = 2.1$ and $\phi_0 = 0.45$, when the Peclet number $\alpha$ is 0, $10^2$, $10^3$, and $10^4$. The size of the system is $400a \times 400a$, with no flux boundary conditions. The snapshots correspond to times $\tau = 0.04$, 0.05, and 0.10, expressed in $10^5 a^2/D$ units. The gray level varies linearly between black and white, corresponding to concentrations $\phi = \phi_{\mathrm{eq}}^A$ and $\phi = \phi_{\mathrm{eq}}^B$, respectively.

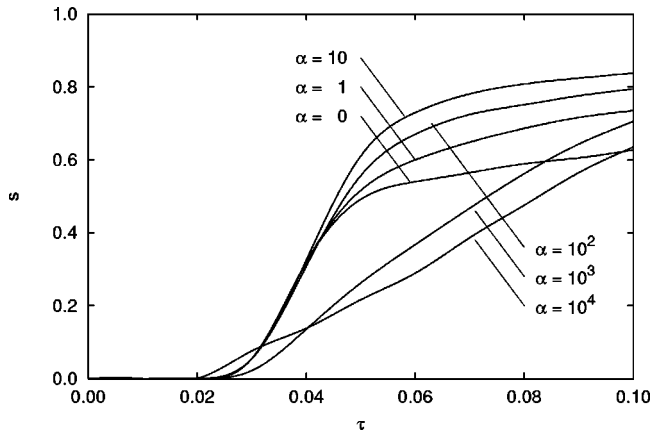


FIG. 4. Separation depth $s$ as a function of time $\tau$ for $\Psi=2.1$ and $\phi_0=0.5$, and with different values of the Peclet number $\alpha$. Results were obtained using $1000a\times1000a$ simulations.

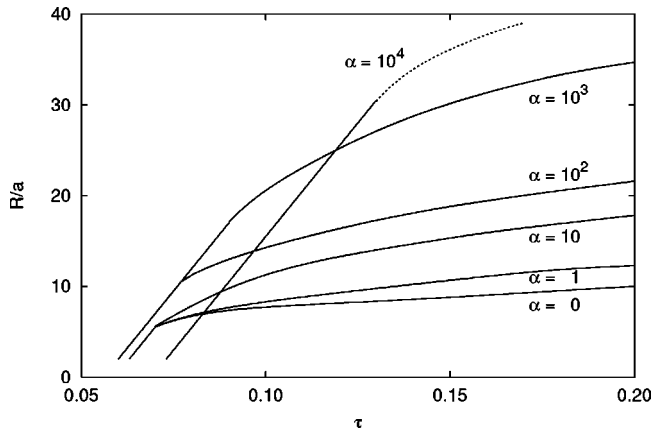


FIG. 6. Equivalent average radius $R$ as a function of time $\tau$ for $\Psi=2.1$ and $\phi_0=0.45$, and with different values of the Peclet number $\alpha$. Results were obtained using $1000a\times1000a$ simulations.

where $A$ is the area of a single-phase domain, while the bracket indicates, as before, volume and ensemble average. The error bars have smaller widths at short times, where the averages were performed over $\sim500$ drops, than at longer times, when drops were larger and the averages were performed over $\sim50$ drops. Again, our results are robust, since identical data points were obtained using $1000a$ and $400a$ size domains. For a given value of $\alpha<10^4$, the equivalent radius grows linearly with time, until it reaches a saturation value, corresponding to the above-mentioned metastable state, after which it grows more slowly. In particular, when $\alpha\leqslant10^2$, we saw that metastable states grow like $t^{1/3}$, while for larger $\alpha$'s they grow more rapidly as $t^n$, with $\frac{1}{3}<n<\frac{1}{2}$ (we do not have enough data to be more specific). On the other hand, when $\alpha>10^4$, the equivalent radius appears to grow linearly until it attains a value which is comparable to the size of the system [39]. The linear growth follows the curve $R\sim10^3a\tau=10^{-2}Dt/a$, and appears to be independent of $\alpha$. Note that for $D\sim10^{-5}$ cm$^2$/s and $a\sim10^{-5}$ cm, we obtain $dR/dt\sim100$ $\mu$/s, in excellent agreement with the experimental results [35].

The growth rate of single-phase domains can be easily estimated using our theoretical model, as $dR/dt=|\mathbf{j}|/\rho$, where $\mathbf{j}$ is the mass flux at the interface. Far from the metastable state, the dominant term of $\mathbf{j}$ is the antidiffusive term in Eq. (14), that is $|\mathbf{j}|\sim\rho(\Delta\phi)[2\phi(1-\phi)\Psi-1](a/l)(D/a)$, where $\Delta\phi$ is the concentration drop across the interface, while $l\sim a/\sqrt{\Psi-2}$ denotes the characteristic thickness of the interface [15]. Therefore, we obtain

$$dR/dt\sim\beta(D/a), \tag{30}$$

with $\beta\sim(\Psi-2)^2$, where we have considered that $(\Delta\phi)_{\rm eq}\sim\sqrt{\Psi-2}$. Equation (30) is in agreement with both experiments and numerical simulations, where $\Psi=2.1$.

The above dimensional analysis can be rewritten substituting Eqs. (24) and (4) into Eq. (30), obtaining

$$\frac{dR}{dt}=k_b\frac{\sigma}{\eta}, \tag{31}$$

where $k_b=\sqrt{\Psi-2}/\alpha$. Equation (31) was obtained by Siggia [18] and San Miguel *et al.* [40], although their predictions, $k_b=0.6$ and $k_b=0.25$, respectively, far overestimate our growth rate results, due to the fact that their analysis is valid for shallow quenches, while ours assumes deep quenches.

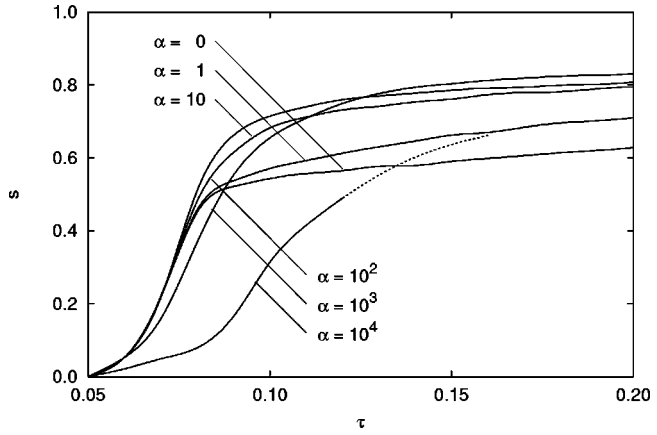


FIG. 5. Separation depth $s$ as a function of time $\tau$ for $\Psi=2.1$ and $\phi_0=0.45$, and with different values of the Peclet number $\alpha$. Results were obtained using $1000a\times1000a$ simulations.

## IV. CONCLUSIONS AND DISCUSSION

In this work we simulated the phase separation occurring when an initially homogeneous liquid binary mixture is deeply quenched into its two-phase region. Our theoretical scheme followed the standard model *H*, where mass and momentum transport are coupled via a nonequilibrium body force, expressing the tendency of the demixing system to minimize its free energy. This driving force, which for sharp interfaces reduces to capillary interaction, induces a convective material flux much larger than its diffusive counterpart, as in a typical case the Peclet number $\alpha$ is of order $10^5$. However, as sharp interfaces form delimiting single-phase domains, a condition of metastable equilibrium is reached, the nonequilibrium driving force (almost) vanishes, and the process becomes diffusion driven.

The set of equations that we used depend on four physical, measurable quantities: the typical interfacial thickness $a$ (proportional to the surface tension), the diffusion coefficient $D$, the kinematic viscosity $\eta/\rho$, and the Margules coefficient

of the mixture, $\Psi$. After rescaling velocity, time scales, and length scales, we obtain a set of two equations [cf. Eqs. (22) and (23)], that can be solved numerically using finite difference techniques. These equations are expressed in terms of two independent parameters, namely, the Margules coefficient and the Peclet number $\alpha$, expressing the ratio between convective and diffusive molar fluxes. Our main conclusions can be summarized as follows.

(1) For critical quenching, the formation of sharp interfaces and the growth of single-phase domains are two successive stages of the phase segregation process when $\alpha < 10^2$, while for $\alpha > 10^3$ they occur simultaneously. For off-critical quenching, the transition between the two stages occurs at larger $\alpha$'s.

(2) Before the formation of sharp interfaces, the equivalent average radius $R$ grows linearly, with $dR/dt \sim 0.01D/a$ for $\Psi = 2.1$ and for all $\alpha$'s, in agreement with both experiments and a first-order dimensional analysis. This linear growth regime ends as sharp interfaces form and the system reaches a metastable state, where diffusion is the dominant mechanism of mass transport. As the Peclet number increases, the transition from a convection-driven to a diffusion-driven process occurs at larger times and larger sizes of the nucleating domains.

(3) After the formation of sharp interfaces, the equivalent average radius $R$ grows in time like $t^{1/3}$ when $\alpha < 10^2$, while it grows somewhat faster (albeit still slower than $t^{1/2}$) for larger $\alpha$'s. The condition of local equilibrium, however, is never reached, showing that the nonequilibrium body force does not vanish even at such late stage of the separation process.

Compared to previous numerical integration of model $H$ equations [19–22], our main contribution is to point out that the linear growth regime cannot continue indefinitely in time, but it reaches an end as sharp interfaces are formed and diffusion becomes the dominant transport mechanism. That shows that the asymptotic scaling regime is not linear, but instead corresponds to the later diffusion-driven stage, thus resolving the apparent contradiction recently pointed out by Grant and Elder [41], who showed that if there exists an asymptotic scaling regime with $R \sim t^n$, then the growth exponent $n$ must be $\leqslant 1/2$, in order to prevent the Reynolds number from diverging at long times. Practically, however, for large values of $\alpha$ the diffusion-driven regime might never be reached, as the nucleating drops would continue to grow linearly until they become large enough that buoyancy dominates surface tension effects, and the mixture separates by gravity. This occurs when the size of the domains becomes equal to the capillary length, $R_{\max} = O(\sigma/g\Delta\rho)$, where $\sigma$ is the surface tension, $g$ the gravity field, and $\Delta\rho$ the density difference between the two separating phases [18], which, for a typical low-viscosity liquid mixture, correspond to $R_{\max} = O(1\ \text{mm})$ [35].

## ACKNOWLEDGMENTS

During this work, N.V. and R.M. were supported in part by the National Science Foundation, Grant No. CTS-9634324.

[1] J. D. Gunton, M. San Miguel, and P. S. Sahni, in *Phase Transition and Critical Phenomena*, edited by C. Domb and J. L. Lebowitz (Academic Press, New York, 1983), Vol. 8, p. 265, and references therein.
[2] Y. C. Chou and W. I. Goldburg, Phys. Rev. A **23**, 858 (1981); A. J. Schwartz, J. S. Huang, and W. I. Goldburg, J. Chem. Phys. **62**, 1847 (1975); **63**, 599 (1975).
[3] N. C. Wong and C. Knobler, J. Chem. Phys. **69**, 725 (1978); Phys. Rev. A **24**, 3205 (1981); E. Siebert and C. Knobler, Phys. Rev. Lett. **54**, 819 (1985).
[4] P. Guenoun, R. Gastaud, F. Perrot, and D. Beysens, Phys. Rev. A **36**, 4876 (1987).
[5] H. Furukawa, Phys. Rev. E **55**, 1150 (1997).
[6] M. Laradji, S. Toxvaerd, and O. G. Mouritses, Phys. Rev. Lett. **77**, 2253 (1996).
[7] W. J. Ma, A. Maritan, J. R. Banavar, and J. Koplik, Phys. Rev. A **45**, R5347 (1992).
[8] G. Leptoukh, B. Strickland, and C. Roland, Phys. Rev. Lett. **74**, 3636 (1995).
[9] F. I. Alexander, S. Chen, and D. W. Grunau, Phys. Rev. B **48**, 634 (1993); S. Chen and T. Lookman, J. Stat. Phys. **81**, 22 (1995); Y. Wu, F. J. Alexander, T. Lookman, and S. Chen, Phys. Rev. Lett. **74**, 3852 (1995).
[10] P. C. Hohenberg and B. I. Halperin, Rev. Mod. Phys. **49**, 435 (1977).
[11] M. Le Bellac, *Quantum and Statistical Field Theory* (Oxford University Press, Oxford, 1991), Sec. 2.4.
[12] J. W. Cahn and J. E. Hilliard, J. Chem. Phys. **28**, 258 (1958); **31**, 688 (1959); J. W. Cahn, *ibid.* **30**, 1121 (1959); Acta Metall. **9**, 795 (1961).
[13] K. Kawasaki, Ann. Phys. (N.Y.) **61**, 1 (1970).
[14] D. Jasnow and J. Viñals, Phys. Fluids **8**, 660 (1996).
[15] R. Mauri, R. Shinnar, and G. Triantafyllou, Phys. Rev. E **53**, 2613 (1996).
[16] N. Vladimirova, A. Malagoli, and R. Mauri, Phys. Rev. E **58**, 7691 (1998).
[17] I. M. Lifshitz and V. V. Slyozov, J. Phys. Chem. Solids **19**, 35 (1961).
[18] E. D. Siggia, Phys. Rev. A **20**, 595 (1979).
[19] T. Koga and K. Kawasaki, Phys. Rev. A **44**, R817 (1991), and references therein.
[20] S. Puri and B. Dunweg, Phys. Rev. A **45**, R6977 (1992).
[21] O. T. Valls and J. E. Farrell, Phys. Rev. E **47**, R36 (1993).
[22] A. Shinozaki and Y. Oono, Phys. Rev. E **48**, 2622 (1993).
[23] H. Furukawa, Phys. Rev. A **31**, 1103 (1985); Physica A **204**, 237 (1994).
[24] O. T. Valls and G. F. Mazenko, Phys. Rev. B **38**, 11 643 (1988).
[25] J. E. Farrell and O. T. Valls, Phys. Rev. B **40**, 7027 (1989); **42**, 2353 (1990); **43**, 630 (1991).
[26] H. Tanaka and T. Araki, Phys. Rev. Lett. **81**, 389 (1998).
[27] P. G. DeGennes, J. Chem. Phys. **72**, 4756 (1980).
[28] J. M. Prausnitz, R. N. Lichtenthaler, and E. Gomes de Azevedo, *Molecular Thermodynamics of Fluid-Phase Equilibria*, 2nd ed. (Prentice-Hall, New York, 1986).
[29] E. A. Guggenheim, *Mixtures* (Oxford University Press, Oxford, 1952).

[30] J. H. Hildebrand and S. E. Wood, J. Chem. Phys. **1**, 817 (1933).
[31] J. D. van der Waals, Z. Phys. Chem., Stoechiom. Verwandtschaftsl. **13**, 657 (1894) [reprinted in J. Stat. Phys. **20**, 200 (1979)].
[32] R. B. Bird, W. E. Stewart, and E. N. Lightfoot, *Transport Phenomena* (Wiley, New York, 1960).
[33] S. R. DeGroot and P. Mazur, *Non-Equilibrium Thermodynamics* (Dover, New York, 1962).
[34] L. Landau and L. Lifshitz, *Fluid Mechanics* (Pergamon, New York, 1953).
[35] R. Gupta, R. Mauri, and R. Shinnar, Ind. Eng. Chem. Res. **38**, 2418 (1999).
[36] P. Bjorstad, Ph.D. dissertation, Stanford University, 1980.
[37] T. M. Rogers, K. R. Elder, and R. C. Desai, Phys. Rev. B **37**, 9638 (1988); K. R. Elder, T. M. Rogers, and R. C. Desai, *ibid.* **38**, 4725 (1988); T. M. Rogers and R. C. Desai, *ibid.* **39**, 11 956 (1989); K. R. Elder and R. C. Desai, *ibid.* **40**, 243 (1989).
[38] H. Tanaka, Phys. Rev. E **51**, 1313 (1995); J. Chem. Phys. **107**, 3734 (1997).
[39] Presumably, even in this case the microdomains will eventually reach a size corresponding to a metastable state, but, due to computational limitations, we could not see it.
[40] M. San Miguel, M. Grant, and J. D. Gunton, Phys. Rev. A **31**, 1001 (1985).
[41] M. Grant and K. R. Elder, Phys. Rev. Lett. **82**, 14 (1999).